

High-Order Numerical Method for One-Dimensional Two-Interface Elliptic Problems

Rong Huang¹, Zhongrong Xiang², Lu Zhang³

¹School of Mathematical Sciences, Guizhou Normal University, Guiyang 550025, China

²School of Mathematical Sciences, Guizhou Normal University, Guiyang 550025, China

³School of Mathematical Sciences, Guizhou Normal University, Guiyang 550025, China

Abstract— This paper presents a high-accuracy spectral element method for one-dimensional elliptic interface problems with two internal discontinuities. We first derive the weak formulation in a standard Sobolev space and its discrete counterpart, and then establish existence and uniqueness of the solution via the Lax–Milgram theorem. We further construct a set of basis functions for the spectral element approximation space and derive the corresponding discrete matrix formulation. Numerical experiments are conducted to validate the effectiveness and spectral accuracy of the proposed method.

Keywords— Elliptic interface problem, spectral element method, well-posedness, algorithm design.

I. INTRODUCTION

Elliptic partial differential equations with discontinuous coefficients, i.e., interface problems, are fundamental in scientific and engineering computing, and their strong and weak solutions have received extensive attention [3]. Early numerical studies focused on homogenization theory and standard finite element methods [6,10], where classical Galerkin approximations guarantee convergence when the mesh aligns with the interfaces [1,2,12]. To handle complex geometries and discontinuous conditions, advanced numerical schemes have been developed. For instance, fast iterative algorithms address the deterioration of the stiffness matrix condition number [9], while unfitted mesh methods such as the immersed interface finite element method [11] and extended mixed finite element method [14] improve flexibility. More recently, the weak Galerkin finite element method, effective for polygonal meshes and curved interfaces, has been widely adopted [13,15].

Although low-order polynomial methods have greatly improved geometric flexibility, spectral methods and the spectral element method are particularly advantageous when extremely high computational accuracy is required, due to their "spectral convergence" (exponential convergence) for smooth or piecewise smooth functions [4,5]. Recently, high-order spectral methods have been successfully applied to elliptic interface problems in various complex domains [7,8]. Since the spectral element method combines the domain decomposition flexibility of the finite element method with the global high accuracy of spectral methods, this paper focuses on the one-dimensional elliptic problem with two internal interfaces. We present a rigorous variational formulation and an efficient discrete algorithm for the proposed spectral element method.

The remainder of this paper is organized as follows. Section 2 derives the weak formulation and its discrete scheme. Section 3 establishes the existence and uniqueness of the solution. Section 4 details the design and implementation of the algorithm. Section 5 presents several numerical examples, and Section 6 concludes the paper with final remarks.

II. WEAK FORM AND DISCRETE SCHEME

In this paper, we consider the following one-dimensional second-order elliptic interface problem:

$$\begin{aligned}
 -(\beta(x)u'(x))' &= f(x), \quad x \in I := (-1,1), \\
 u(\pm 1) &= 0,
 \end{aligned} \tag{2.1}$$

$$[u]_{x=\alpha_i} = 0, \quad \left[\beta \frac{\partial u}{\partial n} \right]_{x=\alpha_i} = 0, \quad i = 1, 2.$$

Here, β is a piecewise smooth function such that

$$\beta(x) = \begin{cases} \beta_1(x), & x \in (-1, \alpha_1), \\ \beta_2(x), & x \in (\alpha_1, \alpha_2), \\ \beta_3(x), & x \in (\alpha_2, 1). \end{cases} \tag{2.2}$$

The jumps across each interface point $x = \alpha_i (i = 1, 2)$ are defined by

$$[u]_{x=\alpha_i} := u|_{x=\alpha_i^-} - u|_{x=\alpha_i^+} = 0; \tag{2.3}$$

$$\left[\beta \frac{\partial u}{\partial n} \right]_{x=\alpha_i} := \beta^- \frac{\partial u}{\partial n} \Big|_{x=\alpha_i^-} - \beta^+ \frac{\partial u}{\partial n} \Big|_{x=\alpha_i^+} = 0. \tag{2.4}$$

We now proceed to derive the variational formulation of problem (2.1) along with its corresponding discrete scheme.

We begin by introducing the relevant Sobolev spaces:

$$\begin{aligned}
 L^2(I) &:= \{v: \int_I v^2 dx < \infty\}, \quad H_0^1(I) := \{v \in L^2(I): v' \\
 &\in L^2(I), v(\pm 1) = 0\},
 \end{aligned}$$

and the standard inner products and the associated norms are defined by

$$(u, v)_{L^2} = \int_I u(x)v(x)dx, \quad \|v\|_{L^2} = \sqrt{(v, v)_{L^2}}, \tag{2.5}$$

$$(u, v)_{H^1} = \int_I (u(x)v(x) + u'(x)v'(x))dx, \quad \|v\|_{H^1} = \sqrt{(v, v)_{H^1}}. \tag{2.6}$$

Furthermore, we define the semi-inner product and the corresponding semi-norm, which is a full norm on $H_0^1(I)$ due to the Poincaré inequality:

$$(u, v)_1 = \int_I u'(x)v'(x)dx, \quad |v|_{H^1} = (v, v)_1^{1/2}. \quad (2.7)$$

Multiplying equation (2.1) by a test function $v \in H_0^1(I)$ and integrating over I , we obtain:

$$\int_I -(\beta(x)u'(x))'v(x)dx = \int_I f(x)v(x)dx.$$

By applying integration by parts on each subdomain and taking into account the homogeneous boundary conditions $v(\pm 1) = 0$ as well as the interface flux continuity conditions in (2.1) which eliminate the boundary and interface jump terms respectively, we obtain that

$$\int_I \beta(x)u'(x)v'(x)dx = \int_I f(x)v(x)dx.$$

The weak formulation of problem (2.1) reads: Find $u \in H_0^1(I)$ such that

$$a(u, v) = f(v), \quad \forall v \in H_0^1(I), \quad (2.8)$$

where the bilinear form $a(\cdot, \cdot)$ and the linear functional $F(\cdot)$ are given by

$$a(u, v) := \int_I \beta(x)u'(x)v'(x)dx,$$

$$F(v) := \int_I f(x)v(x)dx.$$

To formulate the discrete problem, we introduce a finite-dimensional approximation space $V_N \subset H_0^1(I)$. Then, the discrete Galerkin formulation is to find $u_N \in V_N$ such that

$$a(u_N, v_N) = F(v_N), \quad \forall v_N \in V_N. \quad (2.9)$$

III. EXISTENCE AND UNIQUENESS OF SOLUTION

We use the notation $a \lesssim b$ to indicate that $a \leq cb$ for some positive constant c .

Assumption. There exist constants $\beta_{\min}, \beta_{\max} > 0$ such that

$$0 < \beta_{\min} \leq \beta(x) \leq \beta_{\max}, \quad \forall x \in I.$$

Lemma 1 For all $v \in H_0^1(I)$ there holds

$$\|v\|_{H^1} \lesssim |v|_{H^1} \lesssim \|v\|_{H^1}. \quad (3.1)$$

Proof. By the definitions of the semi-norm $|\cdot|_{H^1}$ and the norm

$\|\cdot\|_{H^1}$ in (2.7) and (2.6), we have

$$|v|_{H^1} = \left(\int_I (v'(x))^2 dx \right)^{1/2},$$

$$\|v\|_{H^1} = \left(\int_I (v(x)^2 + (v'(x))^2) dx \right)^{1/2}.$$

The inequality $|v|_{H^1} \leq \|v\|_{H^1}$ is immediate.

For the reverse direction, since $v(\pm 1) = 0$, the Poincaré inequality gives

$$\int_I v^2 dx \lesssim \int_I (v')^2 dx,$$

Which implies

$$\|v\|_{H^1}^2 = \int_I (v^2 + (v')^2) dx \lesssim |v|_{H^1}^2.$$

Hence, we have $\|v\|_{H^1} \lesssim |v|_{H^1}$, which completes the proof.

Lemma 2 The bilinear functional $a(u, v)$ is bounded and positive definite on $H_0^1(I) \times H_0^1(I)$; that is, for all $(u, v) \in H_0^1(I) \times H_0^1(I)$, the following inequalities hold:

$$|a(u, v)| \lesssim |u|_{H^1} |v|_{H^1}, \quad a(u, u) \lesssim |u|_{H^1}^2. \quad (3.2)$$

Proof. From Lemma 1 and the Cauchy-Schwarz inequality, we obtain

$$|a(u, v)| = \left| \int_I \beta(x)u'(x)v'(x)dx \right|$$

$$\leq \beta_{\max} \int_I |u'(x)| |v'(x)| dx$$

$$\leq \beta_{\max} \left(\int_I (u')^2 dx \right)^{1/2} \left(\int_I (v')^2 dx \right)^{1/2} = \beta_{\max} |u|_{H^1} |v|_{H^1}.$$

Moreover, we have

$$a(u, u) = \int_I \beta(x)(u'(x))^2 dx \geq \beta_{\min} \int_I (u')^2 dx = \beta_{\min} |u|_{H^1}^2.$$

This completes the proof.

Theorem 1 If $f \in L^2(I)$, the variational problems (2.8) and (2.9) admit unique solutions $u \in H_0^1(I)$ and $u_N \in V_N$, respectively.

Proof. From Lemma 1 and the Cauchy-Schwarz inequality, we have

$$|F(v)| = \left| \int_I f(x)v(x)dx \right| \leq \|f\|_{L^2} \|v\|_{L^2} \lesssim \|v\|_{L^2} \lesssim |v|_{H^1}.$$

Then, $F(v)$ is a continuous linear functional on $H_0^1(I)$. By combining Lemmas 1-2 with the Lax--Milgram theorem, the desired result follows.

IV. DESIGN AND IMPLEMENTATION OF THE ALGORITHM

In this section, we shall describe how to efficiently solve (2.9). We start by constructing a set of basis functions of the approximation space V_N . Let

$$\varphi_i(t) = L_i(t) - L_{i+2}(t), \quad (i = 0, 1, 2, \dots, N-2), \quad (4.1)$$

where $L_i(t)$ is a Legendre polynomial of degree i .

To facilitate the use of orthogonal polynomials, we define a general affine mapping

$$T_i : (-1, 1) \rightarrow I_i$$

that transforms the reference interval $(-1, 1)$ into the physical subinterval

$$I_i = (x_{i-1}, x_i),$$

Whose length is given by

$$h_i = x_i - x_{i-1}.$$

That is

$$x = T_i(t) = \frac{x_{i-1} + x_i}{2} + \frac{h_i}{2}t, \quad t \in (-1, 1). \quad (4.2)$$

The corresponding inverse mapping is given by:

$$t = T_i^{-1}(x) = \frac{2(x - x_{i-1})}{h_i} - 1, \quad x \in I_i. \quad (4.3)$$

Specifically, for our domain with two interfaces α_1 and α_2 , we set the explicit affine transformations t_1, t_2, t_3 for the three subintervals as follows:

$$\begin{cases} t_1 = \frac{2(x+1)}{\alpha_1+1} - 1, & x \in (-1, \alpha_1), \\ t_2 = \frac{2(x-\alpha_1)}{\alpha_2-\alpha_1} - 1, & x \in (\alpha_1, \alpha_2), \\ t_3 = \frac{2(x-\alpha_2)}{1-\alpha_2} - 1, & x \in (\alpha_2, 1). \end{cases} \quad (4.4)$$

We define the internal basis functions $\phi_{j,i}(x)$ for each subinterval I_j ($j = 1, 2, 3$) using the concise form:

$$\phi_{j,i}(x) = \varphi_i(t_j(x)), \quad x \in I_j, \quad (i = 0, 1, \dots, N-2), \quad (4.5)$$

and $\phi_{j,i}(x) = 0$ for $x \notin I_j$. Here, we denote the subintervals as

$$I_1 = (-1, \alpha_1), \quad I_2 = (\alpha_1, \alpha_2), \quad I_3 = (\alpha_2, 1).$$

Next, we define the basis functions at the interfaces to ensure C^0 -continuity:

$$\begin{aligned} \phi_{N-1}(x) &= \begin{cases} \frac{1+t_1(x)}{2}, & x \in [-1, \alpha_1], \\ \frac{1-t_2(x)}{2}, & x \in (\alpha_1, \alpha_2], \\ 0, & \text{otherwise,} \end{cases} \quad (4.6) \\ \phi_N(x) &= \begin{cases} \frac{1+t_2(x)}{2}, & x \in (\alpha_1, \alpha_2], \\ \frac{1-t_3(x)}{2}, & x \in (\alpha_2, 1], \\ 0, & \text{otherwise.} \end{cases} \quad (4.7) \end{aligned}$$

It is obvious that

$$V_N = \bigcup_{j=1,2,3} \text{span}\{\phi_{j,0}, \phi_{j,1}, \dots, \phi_{j,N-2}\} \oplus \text{span}\{\phi_{N-1}, \phi_N\}$$

We expand the numerical solution u_N as follows:

$$u_N = \hat{u}_{N-1}\phi_{N-1} + \hat{u}_N\phi_N + \sum_{i=0}^{N-2} \hat{u}_{1,i}\phi_{1,i} + \sum_{i=0}^{N-2} \hat{u}_{2,i}\phi_{2,i} + \sum_{i=0}^{N-2} \hat{u}_{3,i}\phi_{3,i}. \quad (4.8)$$

Substituting (4.8) into the discrete formulation and letting v_N run through all basis functions in V_N , the discrete problem reduces to the following linear system:

$$\mathbf{A}\mathbf{u} = \mathbf{f}, \quad (4.9)$$

where

$$\mathbf{A} = \begin{bmatrix} a_{11} & a_{12} & A_{\alpha_1} & A_{\alpha_2} & \mathbf{0} \\ a_{21} & a_{22} & \mathbf{0} & A_{\alpha_2} & A_{\alpha_3} \\ A_{\alpha_1}^T & \mathbf{0} & A_1 & \mathbf{0} & \mathbf{0} \\ A_{\alpha_2}^T & A_{\alpha_2}^T & \mathbf{0} & A_2 & \mathbf{0} \\ \mathbf{0} & A_{\alpha_3}^T & \mathbf{0} & \mathbf{0} & A_3 \end{bmatrix}, \quad \mathbf{u} = \begin{bmatrix} \hat{u}_{N-1} \\ \hat{u}_N \\ U_1 \\ U_2 \\ U_3 \end{bmatrix}, \quad \mathbf{f} = \begin{bmatrix} F_{\alpha_1} \\ F_{\alpha_2} \\ F_1 \\ F_2 \\ F_3 \end{bmatrix}. \quad (4.10)$$

The sub-vectors of \mathbf{u} are $U_j = (\hat{u}_{j,0}, \hat{u}_{j,1}, \dots, \hat{u}_{j,N-2})^T$ for

$j=1, 2, 3$, and the block matrices are defined by

$$A_1 = (a_{ki}^1), \quad A_{\alpha_1} = (a_{\alpha_1,i}^1), \quad A_2 = (a_{ki}^2), \quad A_{\alpha_2} = (a_{\alpha_2,i}^2), \\ A_{\alpha_2} = (a_{\alpha_2,i}^2), \quad A_3 = (a_{ki}^3), \quad A_{\alpha_3} = (a_{\alpha_3,i}^3),$$

where $i, k = 0, 1, \dots, N-2$, and the stiffness entries are given by

$$\begin{aligned} a_{ki}^1 &= \int_{-1}^1 \frac{2}{\alpha_1+1} \beta_1(T_1(t)) \varphi_k'(t) \varphi_i'(t) dt_1, \quad a_{ki}^2 = \int_{-1}^1 \frac{2}{\alpha_2-\alpha_1} \beta_2(T_2(t)) \varphi_k'(t) \varphi_i'(t) dt_2, \\ a_{ki}^3 &= \int_{-1}^1 \frac{2}{1-\alpha_2} \beta_3(T_3(t)) \varphi_k'(t) \varphi_i'(t) dt_3, \\ a_{\alpha_1,i}^1 &= \int_{-1}^1 \frac{1}{\alpha_1+1} \beta_1(T_1(t)) \varphi_i'(t) dt_1, \quad a_{\alpha_1,2}^1 = -\int_{-1}^1 \frac{1}{\alpha_2-\alpha_1} \beta_2(T_2(t)) \varphi_i'(t) dt_2, \\ a_{\alpha_2,2}^2 &= \int_{-1}^1 \frac{1}{\alpha_2-\alpha_1} \beta_2(T_2(t)) \varphi_i'(t) dt_2, \quad a_{\alpha_2,3}^2 = -\int_{-1}^1 \frac{1}{1-\alpha_2} \beta_3(T_3(t)) \varphi_i'(t) dt_3, \\ a_{11} &= \frac{1}{2(\alpha_1+1)} \int_{-1}^1 \beta_1(T_1(t)) dt_1 + \frac{1}{2(\alpha_2-\alpha_1)} \int_{-1}^1 \beta_2(T_2(t)) dt_2, \\ a_{12} &= -\frac{1}{2(\alpha_2-\alpha_1)} \int_{-1}^1 \beta_2(T_2(t)) dt_2 \\ a_{21} &= -\frac{1}{2(\alpha_2-\alpha_1)} \int_{-1}^1 \beta_2(T_2(t)) dt_2, \\ a_{22} &= \frac{1}{2(\alpha_2-\alpha_1)} \int_{-1}^1 \beta_2(T_2(t)) dt_2 + \frac{1}{2(1-\alpha_2)} \int_{-1}^1 \beta_3(T_3(t)) dt_3. \end{aligned}$$

The right-hand side entries are

$$\begin{aligned} F_{\alpha_1} &= \frac{\alpha_1+1}{2} \int_{-1}^1 f(T_1(t)) \frac{1+t}{2} dt_1 + \frac{\alpha_2-\alpha_1}{2} \int_{-1}^1 f(T_2(t)) \frac{1-t}{2} dt_2, \\ F_{\alpha_2} &= \frac{\alpha_2-\alpha_1}{2} \int_{-1}^1 f(T_2(t)) \frac{1+t}{2} dt_2 + \frac{1-\alpha_2}{2} \int_{-1}^1 f(T_3(t)) \frac{1-t}{2} dt_3, \\ (F_j)_i &= \frac{h_j}{2} \int_{-1}^1 f(T_j(t)) \varphi_i(t) dt_j, \quad i = 0, 1, \dots, N-2, \quad j = 1, 2, 3. \end{aligned}$$

V. NUMERICAL EXPERIMENT

To demonstrate the convergence and superior accuracy of our algorithm, we conduct a series of numerical tests in this

section. The problem (2.1) is solved using the spectral element method with varying values of N . All computations are performed using MATLAB R2022a.

Example 1: We consider the one-dimensional elliptic interface problem with two interfaces $\alpha_1 = 0$ and $\alpha_2 = \frac{1}{2}$. The coefficient function $\beta(x)$ is piecewise constant, given by

$$\beta(x) = \begin{cases} 1, & x \in (-1, 0), \\ 2, & x \in (0, \frac{1}{2}), \\ 1, & x \in (\frac{1}{2}, 1), \end{cases}$$

and the right-hand $f(x) = 1$. The exact solution to this problem is

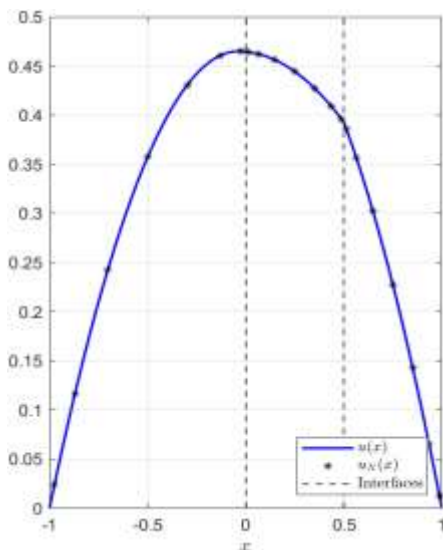


Figure 1: Comparison of the exact solution and the numerical solution with $N = 3$.

Example 2: We consider the one-dimensional elliptic interface problem with two interfaces $\alpha_1 = -0.5$ and $\alpha_2 = 0.5$. The coefficient function $\beta(x)$ is piecewise constant with a large jump, given by

$$\beta(x) = \begin{cases} 1, & x \in (-1, -0.5), \\ 10, & x \in (-0.5, 0.5), \\ 1, & x \in (0.5, 1), \end{cases}$$

and the right-hand side $f(x) = 12x$. The exact solution to this problem is

$$u(x) = \begin{cases} -\frac{x^2}{2} - \frac{x}{28} + \frac{13}{28}, & x \in [-1, 0], \\ -\frac{x^2}{4} - \frac{x}{56} + \frac{13}{28}, & x \in [0, \frac{1}{2}], \\ -\frac{x^2}{2} - \frac{x}{28} + \frac{15}{28}, & x \in [\frac{1}{2}, 1]. \end{cases}$$

In Figure 1, we present a comparison between the exact solution $u(x)$ and the numerical solution $u_N(x)$ for $N = 3$. Figure 2 shows the corresponding absolute error between them.

From Figures 1 and 2, we observe that when $N \geq 3$ the numerical solution achieves an accuracy on the order of 10^{-16} .

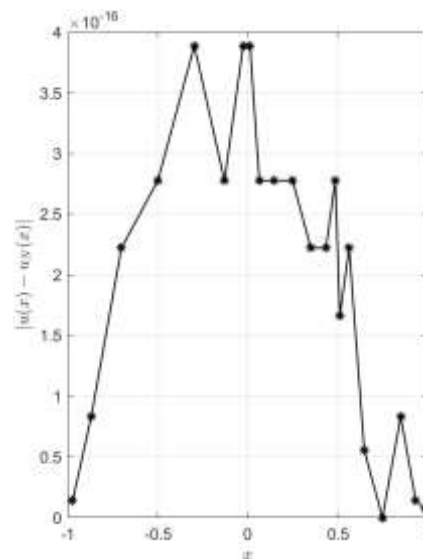


Figure 2: Absolute error distribution between the exact solution and the numerical solution with $N = 3$.

$$u(x) = \begin{cases} -2x^3 + \frac{71}{22}x + \frac{27}{22}, & x \in [-1, -0.5], \\ -0.2x^3 + \frac{71}{220}x, & x \in [-0.5, 0.5], \\ -2x^3 + \frac{71}{22}x - \frac{27}{22}, & x \in [0.5, 1]. \end{cases}$$

In Figure 3, we present a comparison between the exact solution $u(x)$ and the numerical solution $u_N(x)$ for $N = 4$. Figure 4 shows the corresponding absolute error between them.

From Figures 3 and 4, we observe that when $N \geq 4$ the numerical solution achieves an accuracy on the order of 10^{-16} .

Example 3: We consider the one-dimensional elliptic interface problem with two interfaces $\alpha_1 = -\frac{1}{3}$ and $\alpha_2 = \frac{1}{3}$. The coefficient function $\beta(x)$ is piecewise constant, given by

$$\beta(x) = \begin{cases} 1, & x \in (-1, -\frac{1}{3}), \\ 2, & x \in (-\frac{1}{3}, \frac{1}{3}), \\ 5, & x \in (\frac{1}{3}, 1), \end{cases}$$

and the right-hand side $f(x) = 9\pi^2 \sin(3\pi x)$. The exact solution to this problem is

$$u(x) = \begin{cases} \sin(3\pi x), & x \in [-1, -\frac{1}{3}], \\ \frac{1}{2} \sin(3\pi x), & x \in [-\frac{1}{3}, \frac{1}{3}], \\ \frac{1}{5} \sin(3\pi x), & x \in [\frac{1}{3}, 1]. \end{cases}$$

In Figure 5, we present a comparison between the exact solution $u(x)$ and the numerical solution $u_N(x)$ for $N = 60$. Figure 6 shows the corresponding absolute error between them.

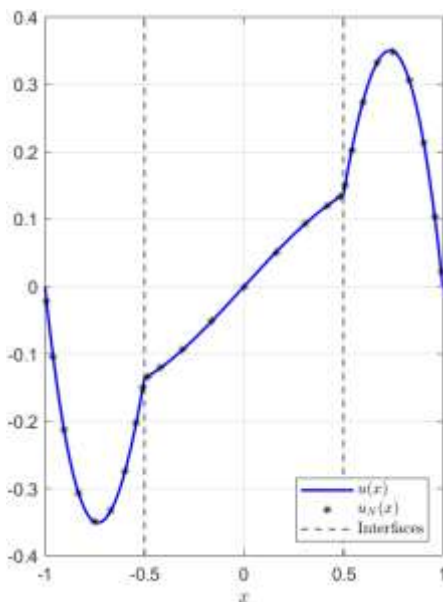


Figure 3: Comparison of the exact solution and the numerical solution with $N = 4$.

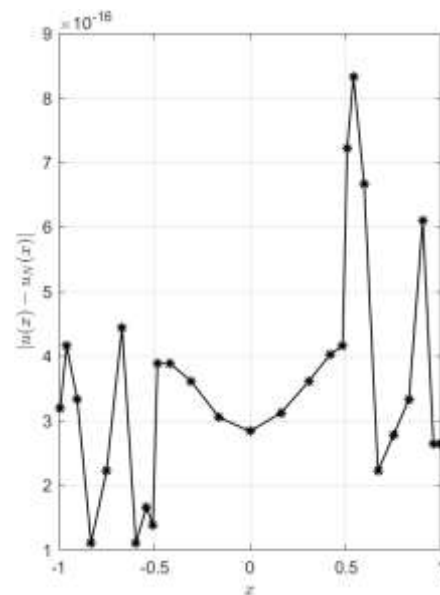


Figure 4: Absolute error distribution between the exact solution and the numerical solution with $N = 4$.

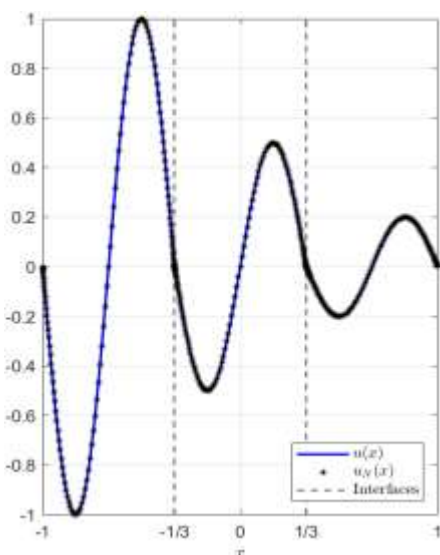


Figure 5: Comparison of the exact solution and the numerical solution with $N = 60$.

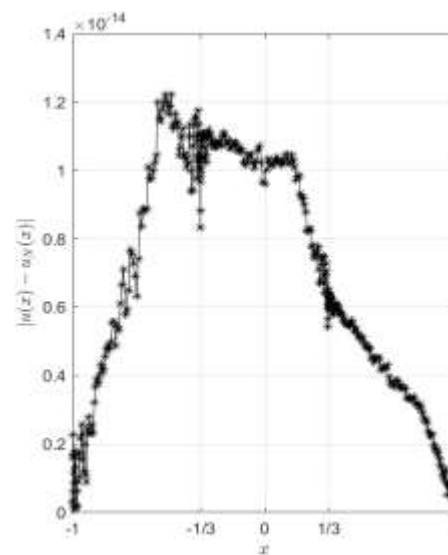


Figure 6: Absolute error distribution between the exact solution and the numerical solution with $N = 60$.

Table 1: Absolute error distribution between the $u(x)$ and the $u_N(x)$ with different N .

N	10	20	30	40	50	60
$ u(x) - u_N(x) $	8.5928e-06	8.5487e-15	1.6993e-14	6.7724e-15	5.5511e-15	1.2212e-14

In Table 1 we present the errors between the exact solution $u(x)$ and the numerical solution $u_N(x)$ for various polynomial degrees N .

From Table 1, it is evident that the accuracy of the numerical solution improves as N increases. When $N \geq 20$, the solution reaches spectral accuracy, stabilizing around 10^{-14} . This convergence behavior and spectral precision are further illustrated in Figures 5 and 6, providing a clear visual confirmation of the algorithm's performance.

VI. CONCLUSIONS

In this paper, we proposed a high-accuracy spectral element method for one-dimensional elliptic interface problems with two internal discontinuities. We established the weak formulation and proved existence and uniqueness of both continuous and discrete solutions via the Lax-Milgram theorem. A set of basis functions was constructed for the spectral element space, leading to a corresponding discrete matrix formulation. Numerical experiments on benchmark problems confirm the spectral accuracy of the method. Future work will extend the approach to two-dimensional interface problems with curved interfaces.

REFERENCES

- [1] S. C. Brenner, L. R. Scott. The mathematical theory of finite element methods. Springer New York, 2008.
- [2] P. G. Ciarlet. The finite element method for elliptic problems. Society for Industrial and Applied Mathematics, 2002.
- [3] L. C. Evans. Partial differential equations. American Mathematical Society, 2022.
- [4] J. Shen, T. Tang, L. L. Wang. Spectral methods: algorithms, analysis and applications. Springer Science & Business Media, 2011.
- [5] G. Kaniadakis, S. Sherwin. Spectral/hp element methods for computational fluid dynamics. American Chemical Society, 2013.
- [6] I. Babuska. The finite element method for elliptic equations with discontinuous coefficients. Computing, 1970, 5(3): 207-213.
- [7] J. An, J. Shen, W. Wang. An Efficient Spectral Method for Elliptic Interface Problems in Two-Dimensional Complex Domains. Journal of Scientific Computing, 2026, 107(1): 5.
- [8] P. Hessari, S. D. Kim, B. C. Shin. Numerical solution for elliptic interface problems using spectral element collocation method. Abstract and Applied Analysis, 2014, 2014(1): 780769.
- [9] Z. Li. A fast iterative algorithm for elliptic interface problems. SIAM Journal on Numerical Analysis, 1998, 35(1): 230-254.
- [10] I. Babuska. Solution of interface problems by homogenization. I. SIAM Journal on Mathematical Analysis, 1976, 7(5): 603-634.
- [11] J. Dolbow, I. Harari. An efficient finite element method for embedded interface problems. International journal for numerical methods in engineering, 2009, 78(2): 229-252.
- [12] J. H. Bramble, J. T. King. A finite element method for interface problems in domains with smooth boundaries and interfaces. Advances in Computational Mathematics, 1996, 6(1): 109-138.
- [13] D. Li, C. Wang, S. Zhang. Weak Galerkin methods for elliptic interface problems on curved polygonal partitions. Journal of Computational and Applied Mathematics, 2024, 450: 115995.
- [14] P. Cao, J. Chen, F. Wang. An extended mixed finite element method for elliptic interface problems. Computers & Mathematics with Applications, 2022, 113: 148-159.
- [15] L. Yang, Q. Zhai, R. Zhang. The weak Galerkin finite element method for Stokes interface problems with curved interface. Applied Numerical Mathematics, 2025, 208: 98-122.